Silicon-based III-V quantum-dot laser for silicon photonics

Manyu Dang, Zizhuo Liu, Ying Lu, Jae-Seong Park, Mengya Liao, Mingchu Tang, Siming Chen, Huiyun Liu

Department of Electronic and Electrical Engineering, University College London, London, WC1E 7JE, United Kingdom
**huiyun.liu@ucl.ac.uk*

Abstract: Monolithic III-V materials grown on Si is a promising platform for silicon photonics. Here, by investigating the laser performance of two conventional III-V quantum structures on Si, namely quantum-dots and quantum-well, we unambiguously demonstrate the excellence and suitability of quantum-dots over quantum-well in silicon-based laser structure and reveal the physical mechanisms underneath, which is attributed to the better tolerance characteristic of quantum-dots for optically detrimental defects. Our work shows that monolithic III-V quantum-dot lasers on Si are the most promising light source for silicon photonics technology. ©2019

OCIS codes: (230.5590) Quantum-well, -wire and -dot devices; (250.5960) Semiconductor lasers; (250.5300) Photonic integrated circuits.

1. Introduction

Silicon photonics technology is preferred to the conventional electronic signal in data transmission, compared with the copper connector, the optical interconnection shows distinguished advantages of high speed, low power consumption, low crosstalk, and simple packaging process. However, Group IV materials such as Si and Ge are inefficient in the light-emitting because of their indirect bandgap [1-2]. Recently, many efforts are targeted at integrating efficient and reliable lasers on Si and silicon on insulator substrate, for which monolithic integration of direct bandgap III-V on Si provides a promising and practically feasible solution. [3]

Nevertheless, the difference in the lattice mismatch between the Group IV and III-V materials inevitably cause challenges for the device-oriented high-quality heteroepitaxial growth, one of which is the formation of high-density threading dislocations (TDs). The propagation of TDs will further produce non-radiative recombination centres in the active region of laser devices, which are detrimental to laser performance and reliability [4,5]. In this work, under the same optimized growth condition, we have fabricated a quantum-dot (QD) laser and a quantum well (QW) laser with the same density of TDs. Via a careful comparison and analysis of the lasing performance for both laser structure, we conclude that on Si, QD laser is superior to QW laser due to the unique properties of QDs, such as efficient carrier capture and high thermal energy barriers preventing the carriers from migrating into defect state.

2. Material growth and fabrication

A 400nm thick APD-free GaAs buffer layer grown on Si on-axis (001) has been employed for the molecular beam epitaxy (MBE) growth of III-V QD and QW growth [6]. The buffer layer comprises a 300nm GaAs following by 4 sets of defect filter layers (DFLs), each set of which is formed by five periods of 10 nm/10 nm $In_{0.18}Ga_{0.82}As$/GaAs strained-layer superlattices (SLSs) separated by a 300 nm GaAs spacing layer. For the QD laser, the active region is 5 layers of InAs/$In_{0.15}Ga_{0.85}As$ dot-in-well (DWELL) structure and each layer of InAs QDs are capped by 6nm $In_{0.15}Ga_{0.85}As$ with 40 nm GaAs spacers. The active region for QW laser consists of the InGaAs/GaAs multi-quantum well (MQW) structure, which is 5 sets of 8 nm $In_{0.15}Ga_{0.85}As$ QW separated by a 40 nm GaAs spacer [7]. These two structures are both grown in the middle of a 1.5 μm n-type lower and a 1.5 μm p-type upper AlGaAs cladding layers. A 300 nm highly doped p-type GaAs contact layer was grown as a final growth step [8,9].

50 μm-wide broad-area laser devices were fabricated using standard photolithography, wet etching, and metallization process [9]. Ni/GeAu/Ni/Au (10/100/30/200 nm) and Ti/Au (40/400 nm) metal contact layers were deposited on the n-GaAs and the p-GaAs contacting layer, respectively. The Si substrates were then thinned to around 120 μm and the laser bars were cleaved into 3 mm long laser cavities, without high-reflection coatings. Finally, the laser bar is mounted onto the copper heatsink, and gold-wire bonding was applied for testing.

3. Result and Discussion

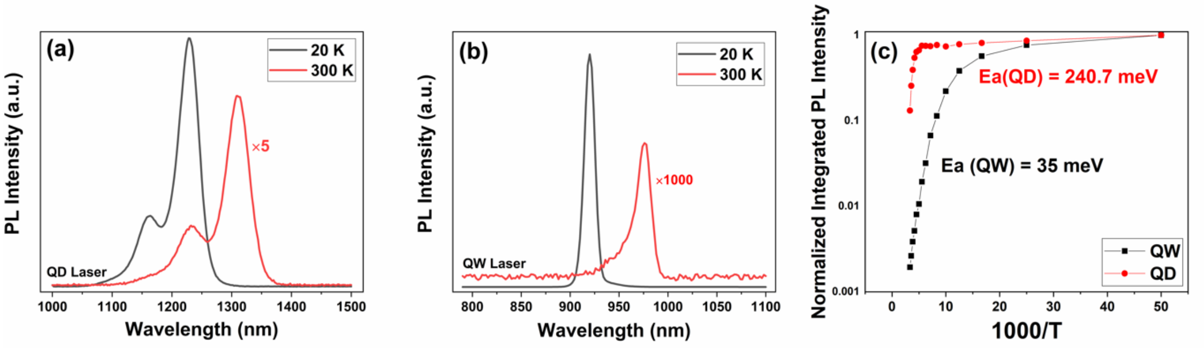

Figure 1. (a) Photoluminescence spectrum of the QD laser at 300K and 20K. (b) Photoluminescence spectrum of the QW laser at 300K and 20K. (c) The integrated PL intensity of the QD and QW laser against the reciprocal of temperature, from 300K to 20K.

The temperature-dependent PL is measured from 20K to 300K by using a 532-nm wavelength laser to excite the samples. It shows that the PL intensity measured at 300K of QD laser device is six times lower than the PL intensity at 20 K as shown in Fig. 1(a). As for the QW sample, the PL intensity shows in Fig. 1(b) at 300 K is about 1000 times lower than that at 20K. This is because the hot carriers have larger possibilities to escape from dots and wells at 300k, which are then trapped into the non-radiative centre in the GaAs barrier [10]. From these measured results, the integrated PL intensity (IPLI) can be deduced under various temperatures, from which the thermal activation energy has been derived from the IPLI according to the Arrhenius Equation. For the QD and QW samples, the thermal activation energy is 240.7meV and 35meV, respectively. Fig. 1(c) shows that the QD sample can maintain a high PL intensity with the temperature increase to 200K while the QW sample quenches rapidly above 50K. Due to the continuous energy state in QWs, any small thermal energy absorption will give a relatively high possibility for carriers escaping from QWs. On the contrary, QD features discrete energy state and benefit from the DWELL structure, it's more difficult for carriers to jump out of the thermal barriers [11].

Fig. 2(a) presents a direct comparison of light-current-voltage (L-I-V) measurements for the QD and QW lasers at room temperature under continuous-wave operation. The measured series resistances of the QD and QW lasers 2.39 ± 0.01 Ω and 2.38 ± 0.02 Ω, respectively. The QD laser shows a low threshold current density of 173 Acm^{-2} and single-facet output power of 100 mW at an injection current of 650 Acm^{-2} without any rollover, whereas the QW laser produces negligible light output and does not show any lasing behaviour at all. A clear super-linear increase of the L-I curve for the QW laser structure is presented in Fig. 2(b), yet the output power rollover at ~1800 Acm^{-2} seems to prevent the device from entering the lasing regime. These results clearly demonstrate the outstanding lasing characteristics of the QD laser monolithically grown on Si compared with this counterpart QW laser with the TDs density of approximately 5×10^{7} cm^{-2} in accordance with a similar experimental of QD and QW laser structures grown on Si with a higher dislocation density of 10^{8} cm^{-2} reported in [12]. Temperature-dependent L-I measurements of QD laser are displayed in Fig. 2(c) under continuous-wave mode from 16 to 65 °C. It is worthwhile to note that, compared with our previous work, the performance of the QD laser monolithically grown on on-axis Si (001) substrate is significantly improved, which can be ascribed to the optimized QD and III-V growth conditions [13].

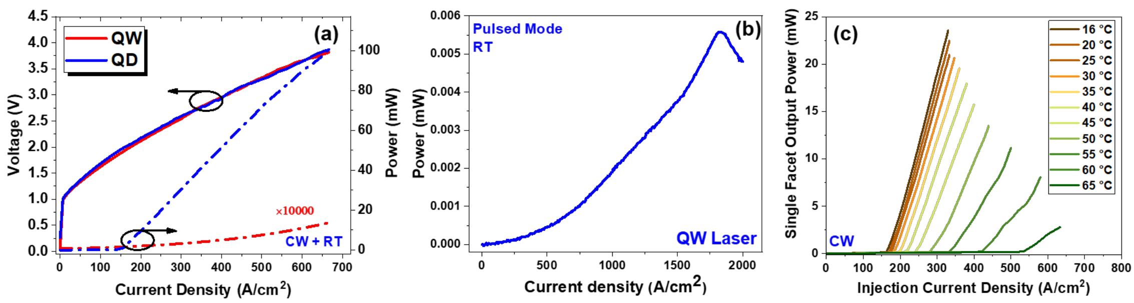

Figure 2. (a) L-I-V measurements of QD and QW lasers monolithically grown on on-axis Si (001) substrate under the same growth conditions at room temperature. (b) L-I measurement of the QW laser with higher injection current under pulsed mode at room temperature. Temperature-dependent L-I measurement of the QD laser under continuous-wave mode.

4. Conclusion

We demonstrate the performance of InAs/GaAs QD and InGaAs/GaAs QW lasers monolithically grown on (001) Si. The QD laser grown on on-axis Si substrate can work with a high operating temperature (65 °C) under continuous-wave mode, while the QW counterpart laser does not show any working operation at room temperature even with higher injection levels. This is due to the carriers in QW are easier to jump out to barrier layer which will be captured by the defect energy state. In the contrast, the carriers in QD are well-confined which need higher energy to escape. The above results clearly show the benefit of using QD as active region in the Si-based III-V laser. Besides, our result also provides a better understanding on the high-performance III-V QD lasers monolithically grown on Si.

Reference

[1] D. Liang et al., “Recent progress in lasers on silicon,” Nature Photonics **4**, 511–517 (2010).

[2] H. Rong et al., "An all-silicon Raman laser," Nature **433**, 292–294 (2005).

[3] S.Chen et al., “Electrically pumped continuous-wave 1.3 µm InAs/GaAs quantum dot lasers monolithically grown on on-axis Si (001) substrates” Optics Express **25**, 4632-4639 (2017).

[4] J. R. Orchard et al., "In situ annealing enhancement of the optical properties and laser device performance of InAs quantum dots grown on Si substrates," Optics Express **24**, 6196-6202 (2016).

[5] K. Böhm and B. Fischer, "Photoluminescence at dislocations in GaAs and InP," Journal of Applied Physics **50**, 5453-5460 (1979).

[6] R. Alcotte et al., "Epitaxial growth of antiphase boundary free GaAs layer on 300 mm Si(001) substrate by metalorganic chemical vapour deposition with high mobility," APL Materials **4**, p. 046101 (2016).

[7] H. Y. Liu et al., "Optimizing the growth of 1.3 µm InAs/InGaAs dots-in-a-well structure," Journal of Applied Physics **93**, 2931-2936 (2003).

[8] Zizhuo Liu, et al. "Origin of defect tolerance in InAs/GaAs quantum dot lasers grown on silicon", Journal of Lightwave Technology (2019).

[9] Chen, S et al, “Electrically pumped continuous-wave III–V quantum dot lasers on silicon”, Nat. Photonics **10**, 307-311 (2016).

[10] Z. Y. Xu et al., "Carrier relaxation and thermal activation of localized excitons in self-organized InAs multilayers grown on GaAs substrates," Physical Review B **54**, 11528-11531 (1996).

[11] O. B. Shchekin, G. Park. et al., "Discrete energy level separation and the threshold temperature dependence of quantum dot lasers," Applied Physics Letters **77**, 466-468 (2000).

[12] A. Y. Liu et al., "Quantum dot lasers for silicon photonics [Invited]," Photonics Research **3**, B1-B9 (2015).

[13] S. Chen et al., “Electrically pumped continuous-wave 1.3 µm InAs/GaAs quantum dot lasers monolithically grown on on-axis Si (001) substrates,” Optics Express **25**, 4632-4639 (2017).